Vehicle-derived emissions and pollution on the road Autovia 2 investigated by rock-magnetic parameters: a case of study from Argentina

DÉBORA C MARIÉ[1,2], MARCOS AE CHAPARRO[1,*], CLAUDIA SG GOGORZA[1], ANA NAVAS[3], ANA M SINITO[1]

1 Instituto de Física Arroyo Seco (UNCPBA)-CONICET, Pinto 399, B7000GHG Tandil, Argentina

2 Universidad Nacional de Mar del Plata (UNMDP)

3 Estación Experimental de Aula Dei, CSIC, Apartado 13034, 50080 Zaragoza, España.

In original form 2008 October 15, revised 2009 April 6

Abbreviated title for page heading:
Vehicle-derived pollution on the road Autovia 2...

* *Name and contact detail of the corresponding author:*

Marcos A.E. Chaparro. Instituto de Física Arroyo Seco (UNCPBA), Pinto 399, B7000GHG Tandil, Argentina.

Phone: +54 2293 439661; Fax: +54 2293 439669

E-mail: chapator@exa.unicen.edu.ar

Abstract

In this work, we carried out a preliminary study of traffic-derived pollutants from primary sources (vehicles), and on roads (paved area), road borders and surroundings areas. The study is focussed on the identification, distribution and concentration of pollutants and magnetic carriers.

The results of magnetic parameters and their analyses suggest that the magnetic signal of vehicle-derived emissions is controlled by a magnetite-like phase, and magnetic grain size estimations reveal the presence of fine particles (0.1-5 μm) that can be inhaled and therefore are dangerous to human health. Results of magnetic susceptibility (about 175×10^{-5} SI) show higher magnetic concentration –*magnetic enhancement*– in the central area of the tollbooth line that is related to higher traffic. In addition, magnetic susceptibility on several roadside soils along 120 km were computed for generating a contour map, such 2-D mapping shows higher magnetic values (100-200 $\times 10^{-5}$ SI) near the edge of the road indicating that magnetic particles emitted by vehicles are accumulated and mainly concentrated within a distance of a couple of meters (1-2 m) along the road. In consequence, magnetic susceptibility parameter seems to be a suitable indicator of traffic-related pollution.

Non-magnetic studies show an enrichment of some trace elements –such as Ba, Cr, Cu, Zn and Pb– associated to traffic pollution. Furthermore, statistical correlations between content of toxic trace metals and magnetic variables support the use of magnetic parameters as potential proxies in this study area.

Keywords: magnetic susceptibility, pollution, roadside soils, toxic trace metals, vehicle emissions

1 Introduction

Different pollution sources involving industry, vehicle and domestic emissions, release in the atmosphere magnetic particles, heavy metals and others compounds that can be incorporated either in the environment or in living organism such as vegetation, animals and human beings.

A major contribution to pollution in urban areas is attributed to traffic, especially emission of vehicles (Palmgren *et al.* 2003). Most of vehicle emissions comprise different fraction particles, that is, ultrafine particles (<30 nm, 30-100 nm) formed in the engine, in the exhaust pipe or immediately after the emission; fine particles (0.1-2 μm) formed by chemical reactions or other processes; and coarse mode (>2 μm) formed mechanically by abrasion of road material, tyres and brake lining (Palmgren *et al.* 2003). These particles can be deeply inhaled and therefore are dangerous to human health, hence respiratory and cardiovascular diseases are among the leading causes of death in many countries (e.g. Pope *et al.* 2002, Knutsen *et al.* 2004, Knox 2006). Some studies indicate a direct relation between particle concentration and health effect increase with decreasing particle grain size (Pope & Dockery 2006).

Magnetic mapping in magnetism has been well accepted for investigating industrial and urban pollution in different environments, such as, soils, rivers/streams and lakes, different vegetation species, and roads (e.g. Hunt *et al*. 1984, Hoffmann *et al.* 1999, Matzka & Maher 1999, Petrovský & Ellwood 1999, Jordanova *et al.* 2003, Amereih *et al.* 2005, Lu *et*

al. 2005, Zhang *et al.* 2006, Kim *et al.* 2007, Chaparro *et al.* 2007, Maher *et al*. 2008). A considerable number of studies have indicated relationships between magnetic parameters and heavy metal concentration based on a genetic relationship from a simultaneous production of both particle sources (e.g. Beckwith *et al.* 1986, Georgeaud *et al.* 1997, Petrovský *et al.* 1998, Knab *et al.* 2001, Spiteri *et al.* 2005, Chaparro *et al.* 2006, 2008).

In this contribution, we carried out a preliminary study of traffic-derived pollutants on roads (asphalt surface), road borders and surroundings areas (soils), as well as on the primary sources (vehicles). The study is mainly focussed on the identification, distribution and concentration of toxic trace metals and magnetic carriers in a road from Argentina and in vehicles using, in particular, various rock-magnetic techniques. Although there are magnetic mapping studies of traffic-related areas, most of them focussed on the influence of pollutants on nearby soils, vegetation and dust particles, being scarce the rock-magnetic studies of primary sources, such as, soot and material from exhaust pipes (e.g. Abdul-Razzaq & Gautam 2001, Lu *et al.* 2005), as well as, from the brake lining system of vehicles. This information can be useful for future investigation on identifying different contamination sources from vehicles and their influence.

2 Material and methods

2.1 Study area and sampling

The study area comprises the road Autovia 2, which is located in the eastern part of the Buenos Aires province (latitude 36º 51’ S, longitude 57º 52’ W, Fig. 1). This road is one of the most important in this province that connects the capital city of Argentina (Buenos

Aires city) with Mar del Plata city; and has a considerable traffic density of about 5500 vehicles per day and reaching about 8000 vehicles per day at the weekends.

Sampling and in situ magnetic susceptibility (κ_{is}) measurements were done in tollbooth sites (Maipu, see Fig. 1) and in various roadside soils –from Maipu to Mar del Plata– along the road Autovia 2. At each measuring way point, several in situ readings were performed and then averaged to avoid non-representative values.

On the other hand, samples were collected from exhaust pipes (inner wall) of several vehicles (gasoline/diesel-soot) as well as from the brake system, road-deposited sediments, asphalt material and roadside soils.

These soils, sediments and soot were carefully sampled using plastic scrapers and tools in order to avoid contamination. Collected samples of scraped material on the road were identified as *CM* (n= 16, samples collected from the tollbooth 1 and 2) and *SM* (n= 8, samples collected from each tollbooths at the vehicle braking/accelerating area), swept material on the road as *LM* (n= 10), soil samples as *MP* (n= 11), road material as *asphalt material* (n= 14), soot samples from vehicles exhaust emission (diesel-powered engines) as *diesel* (n= 11) and (gasoline-powered engines) *gas* (n= 7), and brake system samples as *brake lining material* (n= 4). All samples were air-dried, ground, homogenized and quartered, to pass through a 2 mm sieve.

2.2 Magnetic methods

The collected material was prepared and sub sampled in the laboratory to accomplish several rock-magnetic measurements: magnetic susceptibility (κ), anhysteretic and isothermal remanent magnetisation (ARM and IRM), and stepwise thermal

demagnetisation. Furthermore, several related magnetic parameters, ratios and plots were obtained and analysed. Among them, mass-specific magnetic susceptibility (χ), anhysteretic susceptibility (κ_{ARM}), κ_{ARM}/κ ratio, saturation of IRM (SIRM), S-ratio ($-IRM_{-300mT}/SIRM$), remanent coercivity (H_{cr}) and SIRM/κ ratio were calculated.

Magnetic susceptibility measurements were carried out using a magnetic susceptibility meter MS2, Bartington Instruments Ltd, connected to two sensors: MS2D (for fieldwork) or MS2B (for laboratory work) dual frequency sensor (470 and 4700 Hz). The ARM was imparted superimposing a DC field of 90 μT to an AF of 100 mT, using a partial ARM (pARM) device attached to a shielded demagnetizer Molspin Ltd. IRM (acquisition and backfield) studies were carried out by using an ASC Scientific model IM-10-30 pulse magnetizer. Thermal demagnetisation was done with an ASC Scientific model TD-48 thermal specimen demagnetizer; samples were heated in increasing stepwise temperatures in air; after each step, measurements –remanent magnetisation and magnetic susceptibility– were done for cooled (at room temperature) samples. The remanent magnetisation after each step for ARM, IRM and stepwise thermal demagnetisation studies was measured by a Molspin Ltd. Minispin fluxgate spinner magnetometer.

2.3 Grain size and chemical analysis

Some samples for non-magnetic analyses were homogenised, quartered and prepared for grain size and chemical analyses. Granulometric analysis of sand (>50 μm), silt (2-50 μm) and clay (<2 μm) size fractions were performed using a Coulter laser equipment. To eliminate the organic matter, samples were chemically disaggregated with 10% H_2O_2 heated to 80º C, then stirred and ultrasound was also used to facilitate particle dispersion.

The analysis of the total elemental composition was carried out after total acid digestion with HF (48%) in a microwave oven. The analytical methods are described in detail in Navas & Machín (2002), Navas *et al.* (2008). Samples were analysed for the following 17 elements: Li, K, Na (alkaline), Mg, Ca, Sr, Ba (light metals) and Cr, Mn, Fe, Co, Ni, Cu, Al, Zn, Cd and Pb (heavy metals). Analyses were performed by atomic emission spectrometry using an inductively coupled plasma ICP-OES (solid state detector). Concentrations, obtained after three measurements per element, are expressed in mg/kg and g/kg. Detection limits for the trace elements are: Li: 35 ppb, Cr: 45 ppb, Cu, Zn and Pb: 55 ppb, Co: 40 ppb, Ni: 60 ppb, Cd: 25 ppb.

3 Results and discussion

3.1 In situ magnetic studies

3.1.1 Tollbooth area

Measurements of magnetic susceptibility on the paved area are displayed in Fig. 2. Increases of κ_{is} (higher magnetic concentration) are interpreted as magnetic enhancement if measurements on paved road borders –specially, the paved parking area indicated on the left corner from Fig. 2– are considered as baseline values. Such an assumption is valid taking into account the low vehicles transit by these areas. A similar κ_{is} distribution was found in a German motorway by Hoffmann *et al*. (1999); although in such case of study the traffic density was higher (~24 000 vehicles per day), κ_{is} values on the asphalt surface from this motorway (about 120-130 $\times 10^{-5}$ SI) are comparable with measurements in our study.

From Fig. 2, representative maximum values –about 175 $\times 10^{-5}$ SI– are three times (or more) higher than the baseline values, ~50 $\times 10^{-5}$ SI. The single maxima (e.g. about 250 and 300 $\times 10^{-5}$ SI, Fig. 2) are interpreted as anomalous values associated with inhomogeneities of the asphalt material and/or the presence of Fe-rich material in/under the paved surface. Note that low κ_{is} values are observed towards the road edges.

On the other hand, κ_{is} values on roadside grass area (see in Fig. 2) decrease from the edge of the road. Such decreasing behaviour is also noted in roadside soils along the Autovia 2 (see Sect. 3.1.2 and Fig. 3), which is expected for traffic-related pollutants that can be transported from the road and accumulated on the nearby roadside soils areas. Such behaviour is in agreement with other studies carried out in different countries (e.g. Amereih *et al.* 2005, El-Hasan 2008).

Since the area under study constitutes a compulsory stop for vehicles, it is expected a major contribution and accumulation of pollutants because of the vehicle acceleration and braking than in free-traffic areas. We associate the magnetic enhancement to higher traffic of vehicles, which is particularly noted in the central area of the tollbooth line for site Maipu. This distribution can be related to the available tollbooths for traffic during the year. Central tollbooths –only used by cars– are the most utilised ones, while the others are operational especially on vacations and weekends. Moreover, tollbooths on each road side are mostly transited by heavy duty diesel vehicles (trucks and busses), which are powered by diesel fuel. Thus, an explanation for low values of magnetic susceptibility in such tollbooth areas can be related to diesel soot emission according to the κ values of diesel soot samples (see magnetic properties of diesel/gas soot in Sect. 3.2.2).

3.1.2 Roadside soils

On the other hand, magnetic susceptibility measurements on roadside soils, along the road between Maipu and Mar del Plata, were done and this data-set was computed by using the Origin® 8 Software. Data were converted into a matrix, i.e. a gridding procedure, using the Kriging correlation method (Origin® 8 Software 2007). After applying the gridding procedure, the matrix was used for generating a contour map (Fig. 3).

The spatial distribution (2-D mapping) of magnetic data shows higher values of κ_{is} near the edge of the road, on the contrary, lower values are found moving away from the edge. Such behaviour is expected regarding that pollutant are emitted by vehicles (the only pollution source along the road), transported from the road, and accumulated on the nearby soil. A rather constant magnetic behaviour is expected along the road, but two zones of higher values are noted in Fig. 3. This behaviour is possible if the distance (~120 km) is taking into account and hence terrain level variations (Flanders 1994) may lead to these areas of magnetic accumulation. Another explanation may be related to the influence of the Maipu tollbooth area (0 km) and Mar del Plata city (120 km, Fig. 3). It is possible to note in this figure that both zones are far between them and each one close to the mentioned areas; hence they could induce zones of pollutant accumulation. However, this fact should be confirmed by further and future studies.

Although detailed magnetic measurements on soils from the area are not shown here, the lithogenic/geogenic contribution to the magnetic signal is low. This can be observed in Fig. 2, where κ_{is} values on the grass area far from road centre (about 45-60 m) are about 20×10^{-5} SI. In Fig. 3, low values (about 30-50 $\times 10^{-5}$ SI) are observed within a couple of meters (1-2 m) from the road edge, which is in agreement with the latter conclusion and other previous studies (e.g. Hoffmann *et al*. 1999, Gautam *et al.* 2004, Zhang *et al.* 2006).

3.2 Rock-magnetic studies

3.2.1 Magnetic carriers

Several magnetic parameters and studies are shown in Fig. 4, 5 and 6. They were analysed to identify and characterize the main magnetic carriers. The S-ratio values range from 0.915 to 1 for all samples, except for most of the asphalt samples (0.770-0.873, Fig. 4b), which indicate that magnetic fraction is dominated by ferrimagnetic minerals. Furthermore, the remanent coercivity (H_{cr}) results have a narrow range of variation for swept, scraped and soil samples (31-40 mT); and for vehicles and asphalt material relatively wider between 21 and 36 mT (Fig. 4a).

In Fig. 4a, SIRM/κ and H_{cr} parameters are displayed in a plot, one grouping on the right (specially SM, CM, LM and MP samples) can be appreciated from this plot showing some differences between carriers. On the other hand, differences between most of samples and asphalt samples are clearly observed from another plot, S-ratio versus SIRM/κ (Fig. 4b). This fact is coherent with the nature of the asphalt samples, being constituent material of the pavement, and therefore, different of samples from the pollution (vehicle-derived) source. Most of samples are characterised by higher values of S-ratio and a high dispersion of SIRM/κ values, which is relatively reasonable according to the different kind of samples studied. Magnetic grain size distribution should be taking into account for such a high dispersion, especially, because SIRM/κ parameter is a magnetic carrier and grain size dependent parameter. Nevertheless, it is possible to distinguish that SM, CM and LM samples are well grouped (Fig. 4b), as well as in Fig. 4a, showing low dispersion of S-ratio and SIRM/κ parameters.

The H_{cr} values are coherent with (titano)magnetite range according to Peters & Dekkers (2003), moreover, the presence of magnetite and/or titanomagnetite is confirmed from thermal demagnetisation studies (Fig. 5) as well, where the Curie temperatures of representative samples belong to the range of (titano) magnetite.

Unblocking temperatures (T_U) were identified from changes in the slope of remanent magnetisation. In general, two T_U of ~280ºC and ~580ºC are observed for road (CM, SM and LM) and road-side samples (MP, Fig. 5a, b), though a higher T_U of ~685ºC is observed for an MP sample. Soot and brake lining samples show a first phase at ~135ºC, other at ~330ºC, and the third phase at 580ºC, except for a soot sample at ~685ºC (Fig. 5c). On the other hand, a first phase of 130-180ºC is observed for the asphalt samples, a second one of T_U of ~ 330ºC; and a third phase of higher T_U of 480-530ºC and 630-685ºC (Fig. 5d). The first phases indicate the presence of titanomagnetite, and the second phase (T_U of ~580ºC) corresponds to magnetite (Dankers 1978). The phase of the highest temperatures (>600ºC) may be associated to maghemite and/or hematite.

Magnetic susceptibility measurement at room temperature in thermal demagnetisation studies is particularly used as a tool for monitoring magnetic mineral changes. In these thermal studies, neoformation of (titano) magnetite is not expected, at least in a considerable proportion, according to the magnetic susceptibility results (κ/κ_{RT} versus Temperature, Fig. 5). Neoformation of magnetic minerals (magnetite, maghemite and/or hematite) due to Fe-bearing materials conversion seems to be only possible for diesel samples (Fig. 5c) where the change begins at 280ºC reaching the maximum at 380ºC.

The formation of magnetic particles from the burning of some fossil fuel was pointed out by Flanders (1994). In particular, production of iron oxides from the combustion of diesel

fuel was also reported by Kasper *et al.* (1999), which found that carbonaceous matter preferentially condenses at the surface of the iron oxide nuclei. Abdul-Razzaq & Gautam (2001) reported magnetite in particulate matter collected from diesel engine exhaust; and recently, Kim *et al.* (2007) –on two magnetic extracts– also found iron oxides from diesel vehicle emissions and from the abrasion of brake lining surfaces.

The presence of these magnetic carriers is not only important because of their relationship with heavy metals but also due to their own adverse influence on human health. Such magnetic particles can be inhaled and absorbed in human tissues, having potential implication for many biomedical issues. Among them, human exposure to the strong static magnetic field used in magnetic resonance imaging, as well as to weaker fields produced by the electric power system and cellular phones (e.g. Kirschvink *et al.* 1992). The presence of magnetite in tissues can also cause severe tissue damage, i.e. considerable heat is induced – magnetic thermoablation– when an alternating magnetic field is applied. Such process has not only heating-induced but also cytotoxic effects (Hilger *et al.* 2003).

3.2.2 Magnetic grain size and concentration

Concentration and magnetic grain size of ferrimagnetic carriers (magnetite-like mineral) can be estimated from the King Plot (King *et al.* 1982, Fig. 6). Magnetic concentration can be appreciated from κ parameter in Fig. 6, where the highest values belong to brake lining samples, and the lowest values belong to some asphalt and soot (diesel) samples. The other samples are well grouped showing higher magnetic concentrations, although the grouping is mainly made of scraped, swept and soot (gas) samples, some other samples (asphalt, soil and diesel) can be observed there.

On the other hand, magnetic grain size estimations are made from the calibration lines based on the King's phenomenological model. Such estimations reveal magnetic grain size differences among samples regarding their origin. Note in Fig. 6 that most of scraped and swept samples range from 1 to 5 μm; asphalt samples show two distribution: 0.2-1 μm and 5-20 μm; soil samples range between 0.2 and 1 μm. And as expected, finer particles – between 0.1 and 1 μm– were estimated from one of the main pollution source: soot (gas and diesel) samples. Some diesel and brake samples show exception of higher magnetic grain sizes (1-5 μm).

Results of frequency dependent κ parameter (κ_{FD}%) are mostly below 2%; which indicates scarce or no ultrafine (<0.03 μm) superparamagnetic (SP) ferrimagnetic minerals (Dearing 1994). In particular, lower values were found for scraped (0-2.8%, mean= 1.3%), swept (0-0.3%, mean= 0%), soil (0-2.2%, mean= 0.3%) and brake (0-0.8%, mean= 0.3%) samples than for gas (0-5.6%, mean= 2.4%), diesel (0-3.4%, mean= 1.1%), and asphalt (0-4.7%, mean= 0.7%) samples. Even though mean values of soot (gas and diesel) and asphalt samples are low in general, their ranges may be indicative of admixtures of SP and coarser non-SP grains.

The magnetic grain sizes from our study are in agreement with different fraction particles from vehicle emissions (Palmgren *et al.* 2003). That is, as mentioned above, ultrafine particles (<30 nm, 30-100 nm) formed in the engine by coagulation and condensation of combustion gases; fine particles (0.1-2 μm) formed by chemical reactions after combustion; and coarse mode (>2 μm) formed mechanically by abrasion of road material, tyres and brake lining. Whereas, the presence of relatively coarser magnetic particles in most of

scraped, swept and soil samples may be due to component mixing among different contribution sources, i.e. vehicles emissions, soil material, and asphalt particles.

It is worth mentioning that such magnetic grain size particles reported on here –especially from vehicle emissions– can be easily inhaled, thereafter they can penetrate deep into the respiratory system and their residence time may be very long, up to several months (WHO 2000); in consequence, they may lead to serious hazard to human health.

3.3 Toxic trace metals and granulometric fractions

Determination of the total elemental composition reveals variability among SM, CM and LM samples. A boxplot for 13 selected elements (Li, Sr, Ba, Cr, Cu, Mn, Fe, Al, Zn, Ni, Co, Cd and Pb) and another for granulometric fractions are displayed in Fig. 7 summarising descriptive statistics for each variable. Since these elements are present in the environment, contribution of wind-borne particles from soils should be considered, hence baseline values of elements are displayed in Fig. 7a for comparison. These baseline values were defined from studies of regional soils –Typic, Vertic and Aquic Argiudolls, Typic Natraqualfs, Mollic Natrudalfs, Typic Natraquolls, Typic Natrudolls– according to Lavado *et al*. (2004) and Chaparro *et al*. (2004a).

As can be observed in Fig. 7b, SM, CM and LM samples are dominated by the coarse fraction (sand, about 60%); on the other hand, subordinated fine fractions are about 27% for silt and about 13% for clay contents. However, if scraped (SM and CM) and swept (LM) samples are studied separately, differences are noted. In particular, a balance between fine (54%, silt: ~36% and clay: ~18%) and coarse (sand: ~45%) fractions is observed for scraped samples; but swept samples are dominated by the coarse fraction (sand: ~92%). Although correlations between granulometric fractions and elements are not presented here,

results show positive relationships (R-values: 0.52-0.91) between fine fractions and Li, Cr, Fe, Al, Zn, Co, Cd and Pb.

Concentration of Ba, Cr, Cu, Zn, Cd and Pb (360.7, 50.4, 108.8, 279.6, 1.02 and 115.5 mg/kg respectively, Fig. 7a) are above their corresponding baseline values, considering that traffic is the only pollution source in this area, such element-abundance can be evidently interpreted as an anthropogenic contribution. These elements have previously been reported in other traffic related studies (e.g. Weckwerth 2001, Wang *et al*. 2003, Lin *et al*. 2005).

Based metal additives are originally present in fuels and lubricating oils, e.g. Ba in diesel fuel is used as a smoke suppressant, Mn as an anti-knock agent, Zn, Ca and Mg and other metal based additives are used to minimize the damaging effect of residual complexes – after combustion metal complexes may remain as deposits in the chamber engine– in the corrosion and wear of the engine (Huhn *et al*. 1995, Lim *et al*. 2007). Although these additives are added, manufacturers generally do not provide the elemental composition. Therefore, authors have conducted studies, determining considerable amounts of Ba, Zn, Ca, Fe, Co, Cd and Pb, as well as others –e.g. Li, Sr, Cr, Mn, Ni, Cu– in minor amounts (Lim *et al*. 2007, Wang *et al*. 2003). After combustion, toxic trace metal emission from vehicular sources can be produced by the engine in form of diesel/gas-soot (e.g. Ba, Zn, Ni, Fe, Mn, Cr, Cu, Co, Cd and Pb), general corrosion and engine wear (e.g. Fe and Cr), brake lining system (e.g. Fe, C, O, Al, Si, Ca, S, Sb, Mo, Ba, Zn and Cu, Österle *et al.* 2001, Chan & Stachowiak 2004, Mosleh *et al.* 2004), and tyre wear (e.g. Zn).

As noted in Fig. 7a, there is an enrichment of Ba, Cr, Cu, Zn, Cd and Pb related to the vehicular influence, and therefore these toxic trace metals may be considered as tracers of traffic pollution in the study area. Such result is in agreement with other studies indicating new tracers of vehicle of combustible-powered, that is for example, Ba and Zn (Monaci *et*

al. 2000); Zn, Cr, Ni, Cu and Cd (Weckwerth 2001); Fe and Pb, and a more limited enhancement of Zn, Mn and Ba (Maher *et al*. 2008).

Direct observations of magnetic extracts by scanning electron microscope (SEM, using a JEOL JSM-6460LV microscope) showed different morphologies –spherules and aggregates, agglomerates in a variety of shapes, and (sub)angular particles– and grain sizes that are in agreement with estimated size, i.e. finer submicron agglomerates from diesel soot, (sub)micron agglomerates and spherules from gas soot and coarser micron particles from brake abrasion. Most of determined elements (by chemical analysis), and others (C, O, S, Sb and Ti), were also detected by x-ray Energy Dispersive Spectroscopy (EDS, system EDAX Genesis XM4 - Sys 60). These latter results and SEM observations will be presented elsewhere. This analysis was not only carried out on swept, scraped and soil samples but also on gas, diesel and brake lining material, confirming the production of trace elements from the primary pollution sources: vehicles.

3.4 Relationship between magnetic and chemical variables

The link between magnetic and heavy metal compounds is based on a genetic relationship from a simultaneous production of toxic trace metals and magnetic particles. Most of the statistical analyses in magnetic monitoring have used simple correlation (Pearson's correlation) analysis in order to correlate one-to-one magnetic and chemical variables, obtaining good results as well as statistically non-significant correlations for some magnetic parameters. Some studies showed poor correlations among magnetic susceptibility and heavy metals (e.g. Petrovský *et al.* 1998, Chaparro *et al.* 2004b, Zhang & Yu 2002), whereas alternative magnetic parameters correlated very well (e.g. Georgeaud *et al.* 1998, Chaparro *et al.* 2004a).

Several magnetic (7) and chemical (17) variables were linearly correlated for selected SM, CM and LM samples using the software *Multivariado*. In Table 1, results (R-values) are summarized, and in particular, relevant correlations are highlighted in bold type. These correlations (R>0.5) are of great interest for trace element above their baseline values (discussed above), as noted, Cr and Cd show strong positive correlations with χ (or κ) and ARM; but Ba a moderate negative correlation with ARM. Zn and Pb only show strong and moderate correlations with the κ_{ARM}/κ-ratio, such result was also obtained by Chaparro *et al.* 2004b, 2005 in streams and lakes from Argentina that received pollutants from industrial and urban pollution sources. On the other hand, the metals below their baseline values could be a consequence of natural origin or a mixing between particles of natural and anthropogenic origin. However, Li, Sr, Mn, Fe, Al and Co show moderate and strong positive correlations with χ (or κ), ARM and SIRM. H_{cr} and S-ratio only correlate with Ca, Sr and Mn; and most of correlations between SIRM/κ, κ_{ARM}/κ-ratio and chemical variables are negative.

These results support the existence of relationships between some magnetic and chemical variables. Moreover, the above mentioned conclusions reveal that magnetic concentration parameters (especially χ and ARM) and the magnetic grain size parameter (κ_{ARM}/κ-ratio) can map some toxic trace elements. As noted, concentration of (ferri)magnetic particles and contents of Li, Ba, Cr, Mn, Fe, Al, Co and Cd seem to be associated; and on the other hand, fine grain size ferrimagnetic particles seem to have good affinity with Pb and Zn. Even though possible reasons are beyond the present study, it is worth mentioning that similar correlations were found for this grain size magnetic parameter: κ_{ARM}/κ-ratio in other sites from Argentina (Chaparro *et al.* 2004b, 2005) when magnetic susceptibility yielded poor

correlations. This fact suggests the alternative use of other magnetic parameter to explain such chemical variables.

Although simple correlation results between variables are moderate and strong, allowing the use of magnetic grain size and concentration parameters as indicators of some toxic trace metals emitted by vehicle, further statistical studies should be accomplished to thoroughly investigate links among variables. According to Chaparro *et al.* (2006, 2008), in recent studies, new multivariate statistical techniques –e.g. canonical correlation analysis (CCA), principal coordinate analysis (PCoordA), linear discriminant analysis (LDA) and multivariate analysis of variance (MANOVA)– have been proposed as complementary studies when simple correlation results are not so satisfactory.

4 Conclusions

In this case of study, magnetic susceptibility parameter seems to be a suitable indicator of traffic-related pollution. Results of κ_{is} show magnetic enhancement in the central area of the tollbooth line (on the pavement), and near the edge of the road in soils, allowing as a first-order approach to identify the main areas of interest for pollution in the road Autovia 2. Hence, magnetic enhancement is interpreted as a consequence of deposition and/or movement of pollutants into the asphalt surface and roadside soils.

Results of thermal magnetic studies and remanence parameters indicate the predominance of magnetite-like phases that control the magnetic signal of vehicle-derived emissions. Although all collected samples: scraped, swept, soil, asphalt material, brake lining and soot samples show a similar magnetic behaviour, it is possible to discriminate among them according to their magnetic concentration and features. Magnetic grain size estimations

from our study are in most samples below 5 μm, and finer (0.1-2 μm) for soot samples; comprising fine particles that can be deeply inhaled and therefore can potentially lead to dangerous respiratory and cardiovascular diseases.

The sources of pollution are vehicles that produce soot particles from exhaust and other solid particles generated by tyres, brake-lining, engine corrosion and abrasion of vehicles surfaces. Elemental composition analysis confirmed the presence and enrichment of some toxic trace metal, such as Ba, Cr, Cu, Zn, Cd and Pb, which may be considered as tracers of traffic pollution in the study area. Moreover, magnetic studies on brake lining and soot samples show a strong magnetic signal supporting the production of magnetic particles (in addition to toxic trace metals) from the primary sources.

The co-existence of both metal and magnetic particles is supported from correlation analysis, selected magnetic and chemical variables show moderate and strong correlations (R-values from 0.55 to 0.83), hence the magnetic concentration parameters (χ or κ and ARM) and magnetic grain size parameter (κ_{ARM}/κ-ratio) are potential indicators to map some toxic trace elements: Ba, Cr, Zn, Cd and Pb.

Acknowledgements

The authors thank the CONICET, UNCPBA, UNMDP, and Estación Experimental de Aula Dei (CSIC). The authorities (Ing. M. Vincent) and staff of the tollbooth Autovia 2 (Peaje Maipu) are also thanked for their useful help to carry out the sampling. D. Marié was supported by two Fellowships (2005-2006, 2008) from the Comisión de Investigaciones Científicas de la Pcia. de Buenos Aires (CICPBA) and the Inter U program. Financial support was also received from a PICT-2005 of the ANPCYT, project No. 38050. The authors thank to M. Chaparro for his

assistance. They also appreciate the contribution of both reviewers for their detailed revisions and valuable comments.

References

Abdul-Razzaq W, Gautam M (2001) Discovery of magnetite in the exhausted material from a diesel engine. App Phys Lett, 78: 2018-2019

Amereih S, Meisel T, Scholger R, Wegscheider W (2005) Antimony speciation in soil samples along two Austrian motorways by HPLC-ID-ICP-MS, J. Environ. Monit, 7, 1200-1206.

Beckwith P, Ellis J, Revitt D, Oldfield F (1986) Heavy metal and magnetic relationships for urban source sediments. Phys. Earth Planet. Int., 42, 67-75.

Chan D, Stachowiak GW (2004) Review of automotive brake friction materials. Proc. Instn Mech. Engrs., 218(D):953-966

Chaparro MAE, Bidegain JC, Sinito AM, Gogorza CS, Jurado S (2004a) Magnetic Studies Applied to Different Environments (Soils and Stream-Sediments) from a Relatively Polluted Area in Buenos Aires Province, Argentina. Environ. Geol., 45 (5): 654-664.

Chaparro MAE, Bidegain JC, Sinito AM, Jurado S, Gogorza CS (2004b) Relevant magnetic parameters and heavy metals from relatively polluted stream-sediments—spatial distribution along a cross-city stream in Buenos Aires Province, Argentina. Stud Geophys Geod 48(3):615–636

Chaparro MAE, Lirio JM, Nuñez H, Gogorza CSG, Sinito AM (2005) Preliminary magnetic studies of lagoon and stream sediments from Chascomus area (Argentina)—magnetic parameters as pollution indicators and some results of using an experimental method to separate magnetic phases. Environ Geol 49(1):30–43

Chaparro MAE, Gogorza CSG, Chaparro MAE, Irurzun MA, Sinito AM (2006) Review of magnetism and heavy metal pollution studies of various environments in Argentina. Earth Planets Space 58(10):1411-1422

Chaparro MAE, Nunez H, Lirio JM, Gogorza CGS, Sinito AM (2007) Magnetic screening and heavy metal pollution studies in soils from Marambio station, Antarctica. Antarctic Science, 19 (3), 379–393.

Chaparro MAE, Chaparro MAE, Marinelli C, Sinito AM (2008) Multivariate techniques as alternative statistical tools applied to magnetic proxies for pollution: cases of study from Argentina and Antarctica. Environ Geol., 54, 365–371.

Dankers PHM (1978) Magnetic properties of dispersed natural iron-oxides of known grain-size. PhD thesis, State University of Utrecht, 142 pp. [Unpublished.]

Dearing JA (1994) Environmental magnetic susceptibility: using the Bartington MS2 system. Kenilworth. Chi Publishing, 54 pp.

El-Hasan T (2008) The detection of roadside pollution of rapidly growing city in arid region using the magnetic proxies. Environ Geol 54:23–29

Flanders PJ (1994) Collection, measurement, and analysis of airborne magnetic particulates from pollution in the environment. J. Appl. Phys,, 75(10):5931-5936

Gautam P, Blaha U, Appel E, Neupane G (2004) Environmental magnetic approach towards the quantification of pollution in Kathmandu urban area, Nepal. Phys Chem Earth, 29:973-984

Georgeaud VM, Rochette P, Ambrosi JP, Vandamme D, Williamson D (1997) Relationship between heavy metals and magnetic properties in a large polluted catchment: the Etang de Berre (South of France). Phys Chem. Earth, 22(1–2), 211–214.

Hilger I, Fruhauf S, Linss W, Hiergeist R, Andra W, Hergt R, Kaiser W (2003) Cytotoxicity of selected magnetic fluids on human adenocarcinoma cells. J Magnetism Magnetic Materials, 261:7–12

Hoffmann V, Knab M, Appel E (1999) Magnetic susceptibility mapping of roadside pollution, J. Geochem. Int., 66 (1-2), 313–326.

Huhn G, Schulz H, Staerk HJ, Toelle R, Scheuermann G (1995) Evaluation of regional heavy metal deposition by multivariate analysis of element contents in pine tree barks. Water Air Soil Poll. 84: 367-383.

Hunt A, Jones J, Oldfield F (1984) Magnetic measurements and heavy metals in atmospheric particulates of anthropogenic origin. Sci. Total Environ., 33, 129-139.

Jordanova NV, Jordanova DV, Veneva L, Andorova K, Petrovský E (2003) Magnetic response of soils and vegetation to heavy metal pollution—A case of study, Environ. Sci. Tech., 37, 4417–4424.

Kasper M, Sattler K, Siegmann K, Matter U, Siegmann HC (1999) The influence of fuel additives on the formation of carbon during combustion. J. Aerosol Sci., 30(2):217-225

Kim W, Doh S-J, Park Y-H, Yun S-T (2007) Two-year magnetic monitoring in conjunction with geochemical and electron microscopic data of roadside dust in Seoul, Korea. Atm. Environ., 41: 7627-7641

King J, Banerjee SK, Marvin J & Özdemir Ö (1982) A comparison of different magnetic methods for determining the relative grain size of magnetite in natural materials: Some results from lake sediments. Earth Planet. Sci. Lett., 59, 404-419.

Knab M, Appel E, Hoffmann V (2001) Separation of the anthropogenic portion of heavy metal contents along a highway by means of magnetic susceptibility and fuzzy c-means clusteranalysis. Eur. J. Environ. Eng. Geophys., 6: 125-140.

Knox EG, 2006. Roads, railways and childhood cancers. Journal of Epidemiology and Community Health 60, 136–141.

Knutsen S, Shavlik D, Chen LH, BeesonWL, Ghamsary M, Petersen F, 2004. The association between ambient particulate air pollution levels and risk of cardiopulmonary and all-cause mortality during 22 years follow-up of a non-smoking cohort. Results from the AHSMOG study. Epidemiology 15, S45.

Kirschvink JL, Kobayashi-Kirschvink A, Woodford BJ (1992). Magnetite biomineralization in the human brain. Proc. Natl. Acad. Sci. USA 89:7683

Lavado RS, Zubillaga MS, Alvarez R, Taboada MA (2004) Baseline levels of potentially toxic elements in Pampas soils. Soil & Sediment Contamination, 13, 427-437.

Lim MCH, Ayodo GA, Morawska L, Ristovski ZD, Jayaratne ER (2007) The effects of fuel characteristics and engine operating conditions on the elemental composition of emissions from duty diesel buses. Fuel, 86: 1831-1839.

Lin C-C, Chen S-J, Huang KL (2005) Characteristics of metals in nano/ultrafine/fine/coarse particles collected beside a heavily trafficked road. Environ. Sci. Tech., 39 (21): 8113-8122.

Lu S-G, Bai S-Q, Cai J-B, Xu C (2005) Magnetic properties and heavy metal contents of automobile emission particulates. J. Zhejiang Univ. SCI., 6B(8): 731-735.

Maher BA, Moore C, Matzka J (2008) Spatial variation in vehicle-derived metal pollution identified by magnetic and elemental analysis of roadside tree leaves. Atm. Environ., 42, 364-373.

Matzka J, Maher BA (1999) Magnetic biomonitoring of roadside tree leaves: identification of spatial and temporal variations in vehicle derived particulates, Atm. Environ., 33, 4565–4569.

Monaci F, Moni F, Lanciotti E, Grechi D, Bargagli R (2000) Biomonitoring of airborne metals in urban environments: new tracers of vehicle emission, in place of lead. Environ. Poll. 107: 321-327.

Mosleh M, Blau PJ, Dumitrescu D (2004) Characteristics and morphology of wear particles from laboratory testing of disk brake materials. Wear, 256:1128-1134

Navas A, Machín J (2002) Spatial distribution of heavy metals and arsenic in soils of Aragón (NE Spain): controlling factors and environmental implications. App. Geochem., 17: 961-973.

Navas A, López-Martinez J, Casas J, Machín J, Durán JJ, Serrano E, Cuchí JA, Mink S (2008). Soil characteristics on different lithological substrates in South Shetland Islands, Maritime Antarctica. Geoderma, 144:123-139.

Origin® 8 Software, 2007. Origin 8 User Guide. Northampton, MA: OriginLab Corporation. First edition, pp. 545.

Österle W, Griepentrog M, Gross Th, Urban I (2001) Chemical and microstructural changes induced by friction and wear of brakes. Wear, 251:1469-1476

Palmgren F, Waahlin P, Kildesó J, Afshari A, Fogh CL (2003) Characterisation of particle emissions from the driving car fleet and the contribution to ambient and indoor particle concentrations. Phys. Chem. Earth, 28: 327-334.

Peters C, Dekkers MJ (2003) Selected room temperature magnetic parameters as a function of mineralogy, concentration and grain size. Phys. Chem. Earth, 28: 659-667.

Petrovský E, Kapicka A, Zapletal K, Sebestová E, Spanilá T, Dekkers MJ, Rochette P (1998) Correlation between magnetic properties and chemical composition of lake sediments from northern Bohemia. Preliminary study. Phys Chem Earth (A) 23(9-10):1123-1126

Petrovský E, Elwood B (1999) Magnetic monitoring of air, land and water pollution. In: Quaternary Climates, Environment and Magnetism (Eds. BA Maher, R Thompson), Cambridge University Press, 279-322

Pope CA, Burnett RT, Thun MJ, Calle EE, Krewski D, Kazuhiko I, Thurston GD (2002) Lung cancer, cardiopulmonary mortality, and long-term exposure to fine particulate air pollution. J American Medical Association 287, 1132–1141.

Pope CA, DockeryDW (2006) Health effects of fine particulate air pollution: lines that connect. J Air Waste Manage Assoc 56:709–742

Spiteri C, Kalinski V, Rösler W, Hoffmann V, Appel E, MAGPROX team (2005) Magnetic screening of a pollution hotspot in the Lausitz area, Eastern Germany: correlation analysis between magnetic proxies and heavy metal contamination in soils. Environ Geol 49:1–9

Wang Y-F, Huang K-L, Li C-T, Mi H-H, Luo J-H, Tsai P-J (2003) Emissions of fuel metals content from a diesel vehicle engine. Atm. Environ. 37: 4637-4643.

Weckwerth G (2001) Verification of traffic emitted aerosol components in the ambient air of Cologne (Germany). Atm. Environ. 35: 5525-5536.

WHO (2000) Air quality Guidelines for Europe, second ed., Particulate matter WHO Regional Publications, Europe Series, No. 91. Copenhagen, Denmark, 186 pp.

Zhang W, Yu L (2002) Relationships between magnetic properties and heavy metals in intertidal sediments of the Yangtze Estuary, China. Quaderni di Geofisica, 26:195−197.

Zhang C, Huang B, Li Z, Liu, H (2006) Magnetic properties of highroad-side pine tree leaves in Beijing and their environmental significance. Chinese Sci. Bull., 51(24):3041-3052

Figure Legends

Fig. 1. Map of Buenos Aires province (Argentina), the road Autovia 2 and tollbooth sites.

Fig. 2. Measurements of in situ magnetic susceptibility (κ_{is}) on the paved area (black colour) and on the roadside grass area (gray colour). A profile across the road Autovia 2 is shown in Maipu tollbooth area. Numbers (bottom) correspond to each tollbooth.

Fig. 3. Contour map of in situ magnetic susceptibility (κ_{is}) on roadside soils along the road Autovia 2. High values of κ_{is} are observed near the road edge.

Fig. 4. Magnetic properties for all samples: sediments, soils, diesel/gasoline soot, asphalt and brake samples. (a) Biplot of SIRM/κ vs. remanent coercivity (H_{cr}); (b) Biplot of S-ratio vs. SIRM/κ.

Fig. 5. Stepwise thermal demagnetisation (black colour) and normalised magnetic susceptibility (gray colour) measured at room temperature (after each step). Measurements for selected samples of: a) road sediments, b) road-side soils, c) diesel soot and brake lining material, d) asphalt material.

Fig. 6. κ_{ARM} vs. κ (King plot, King *et al*. 1982) for all samples: sediments, soils, diesel/gasoline soot, asphalt and brake lining samples.

Fig. 7. (a) Elemental composition and (b) grain size analysis of selected samples (*n= 12*; 5 samples SM, 2 samples CM and 5 samples LM). Variability of some selected element contents (in mg/kg for all elements, except for Fe and Al in g/kg). The box delineates interquartile range 25-75%, and the horizontal line in box indicates the median. Minimum and maximum values are shown using whiskers, as well as the mean value with an open square. The circles correspond to baseline values of regional soils from Buenos Aires province (Lavado *et al*. 2004, Chaparro *et al*. 2004a).

Table Titles

Table 1. Statistical results (*n*= 12). Linear correlation (R-values) between magnetic and chemical variables.

Figures

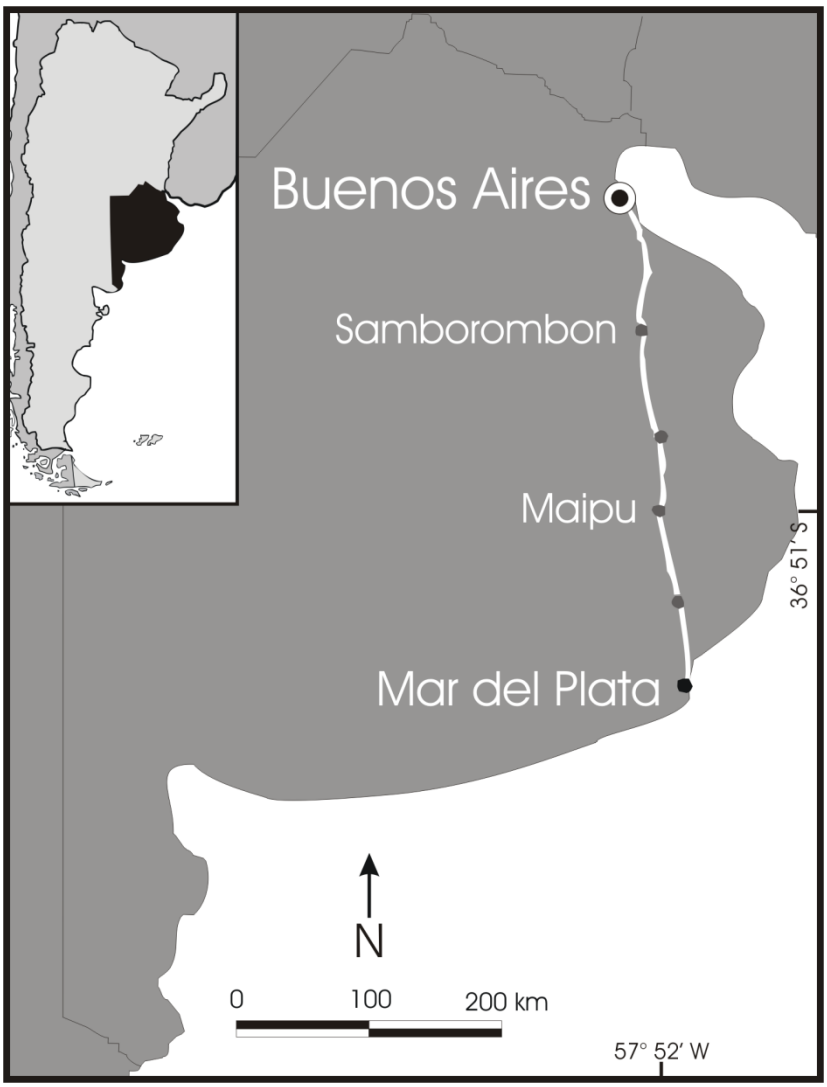

Fig. 1

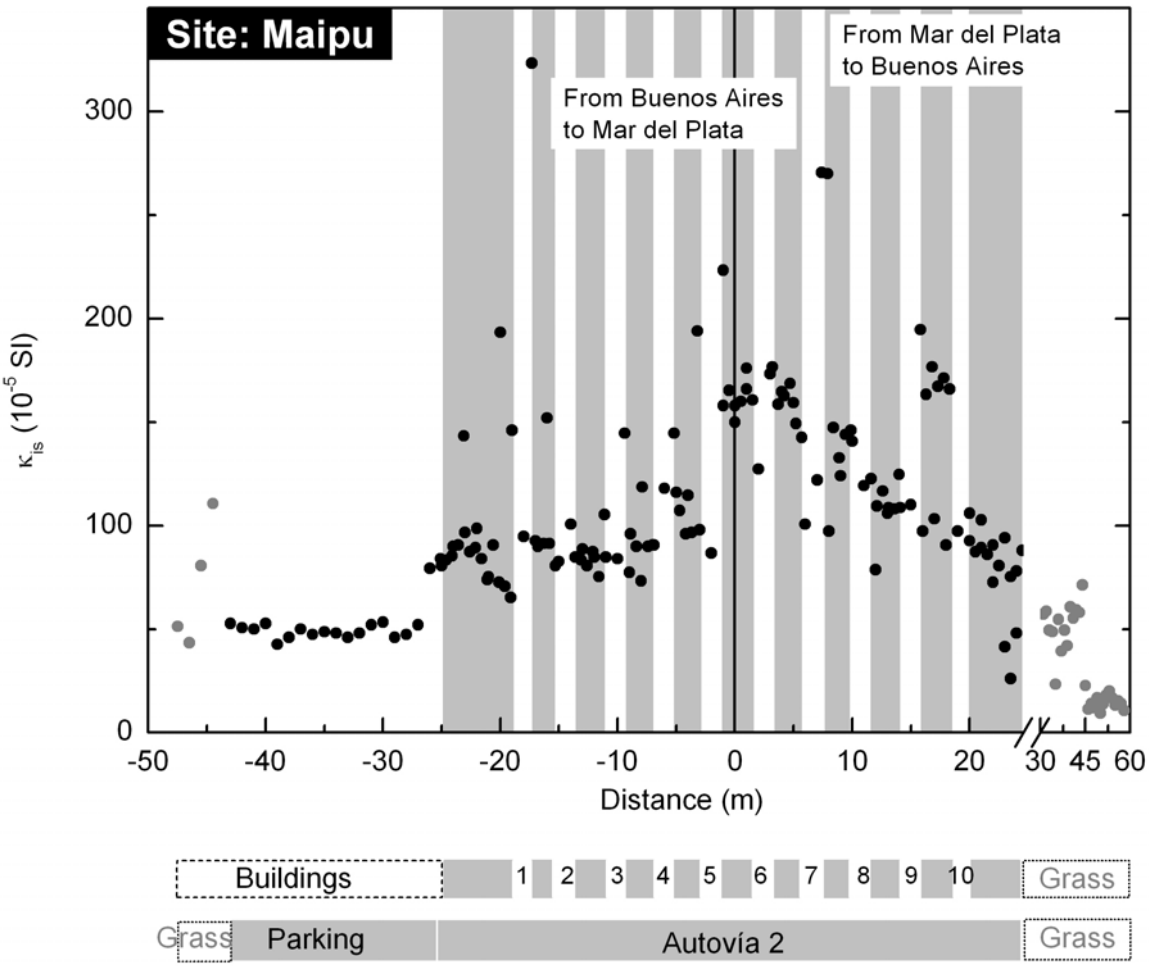
Site: Maipu
From Buenos Aires
to Mar del Plata
From Mar del Plata
to Buenos Aires
κ_{is} (10^{-5} SI)
300
200
100
0
-50
-40
-30
-20
-10
0
10
20
30
45
60
Distance (m)
Buildings
1
2
3
4
5
6
7
8
9
10
Grass
Grass
Parking
Autovía 2
Grass

Fig. 2

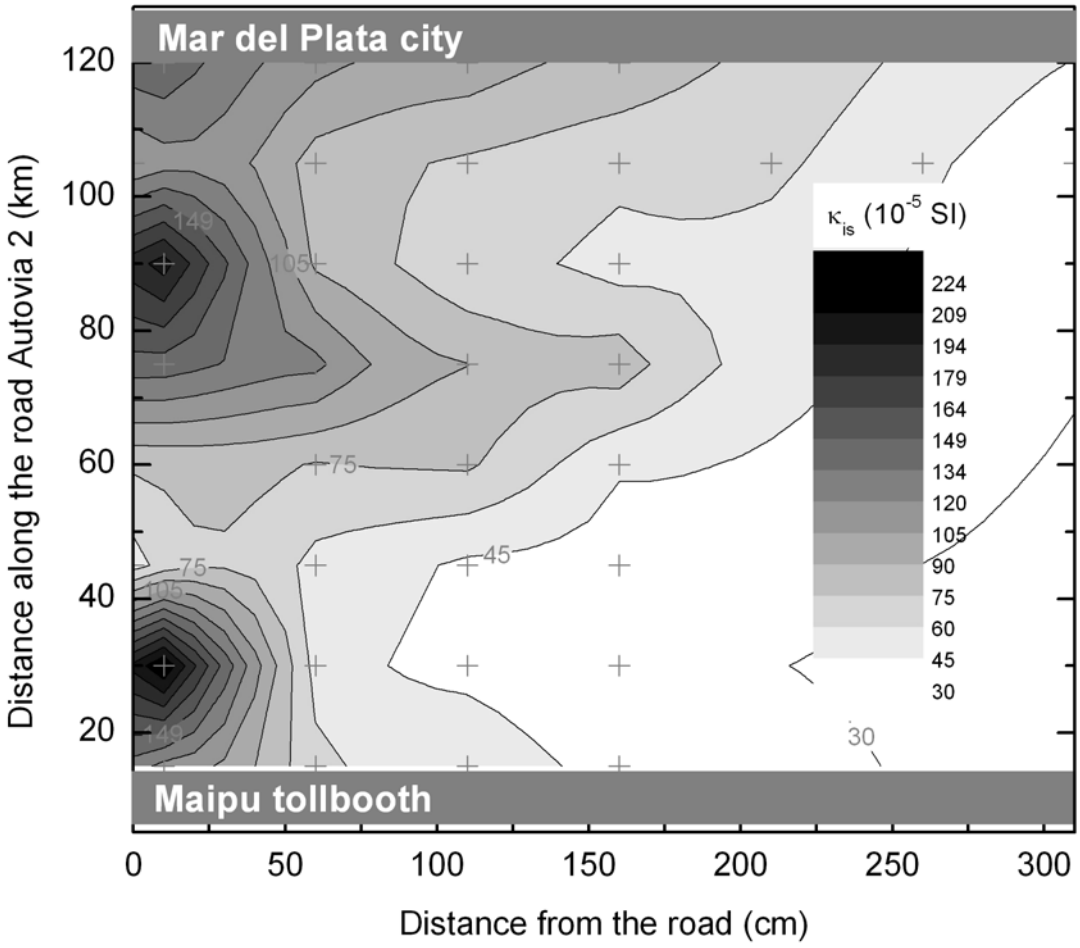
Mar del Plata city
Maipu tollbooth
Distance along the road Autovia 2 (km)
Distance from the road (cm)
κis (10-5 SI)
224
209
194
179
164
149
134
120
105
90
75
60
45
30
120
100
80
60
40
20
0
50
100
150
200
250
300

Fig. 3

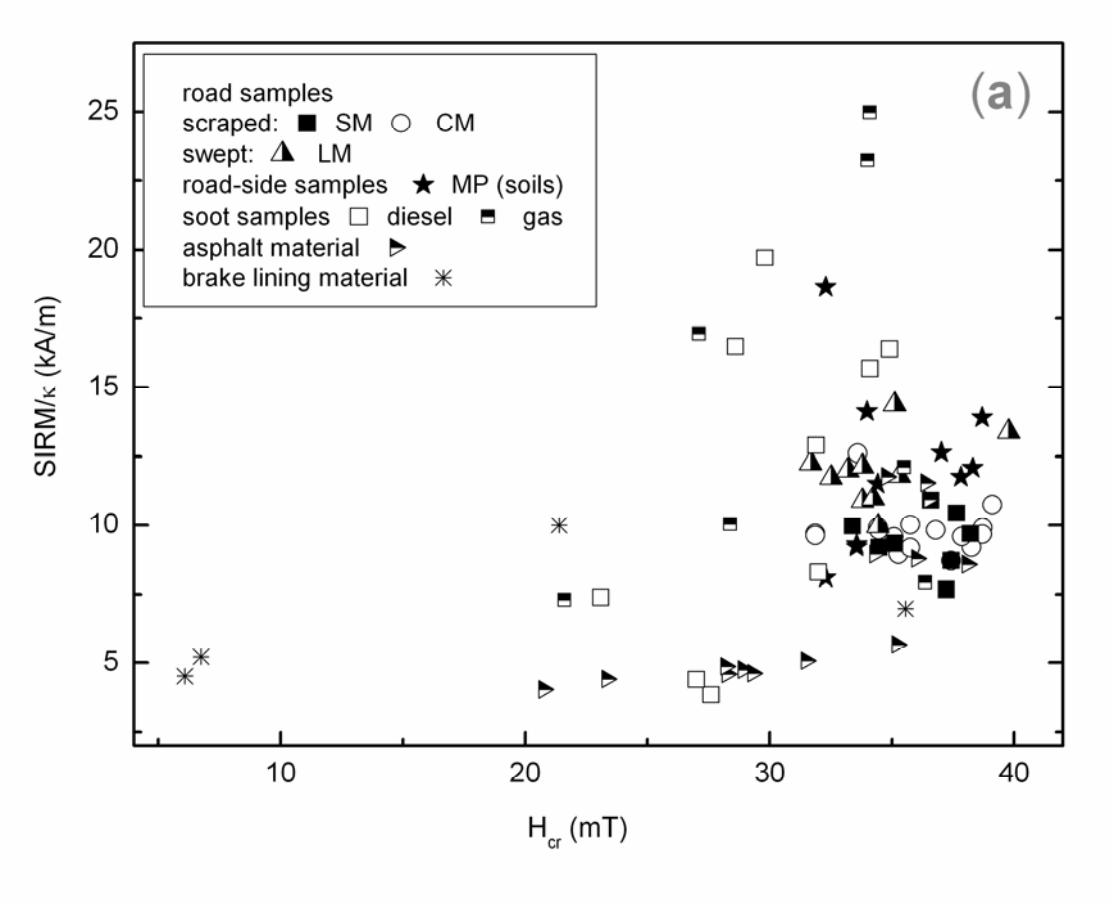
road samples
scraped: SM CM
swept: LM
road-side samples MP (soils)
soot samples diesel gas
asphalt material
brake lining material
(a)
SIRM/κ (kA/m)
H_cr (mT)
25
20
15
10
5
10
20
30
40

Fig. 4a

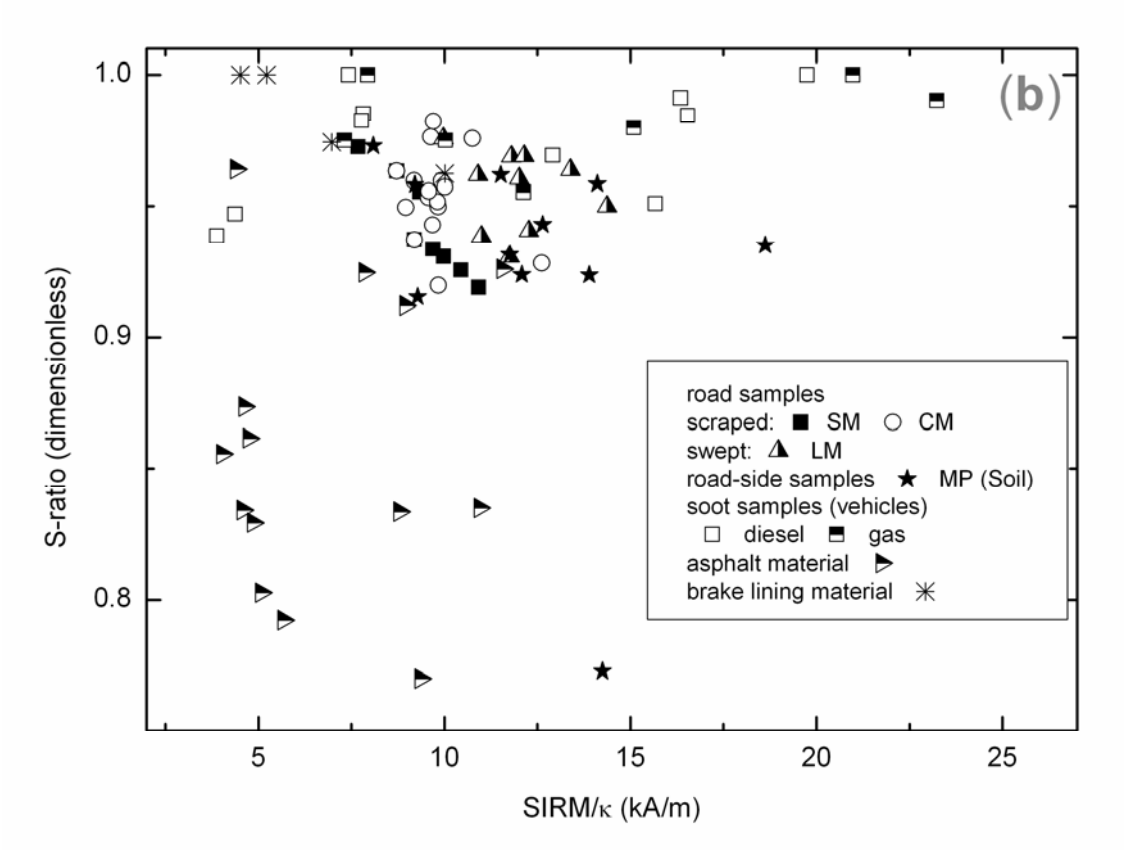
(b)
S-ratio (dimensionless)
1.0
0.9
0.8
5
10
15
20
25
SIRM/κ (kA/m)
road samples
scraped: SM CM
swept: LM
road-side samples MP (Soil)
soot samples (vehicles)
diesel gas
asphalt material
brake lining material

Fig. 4b

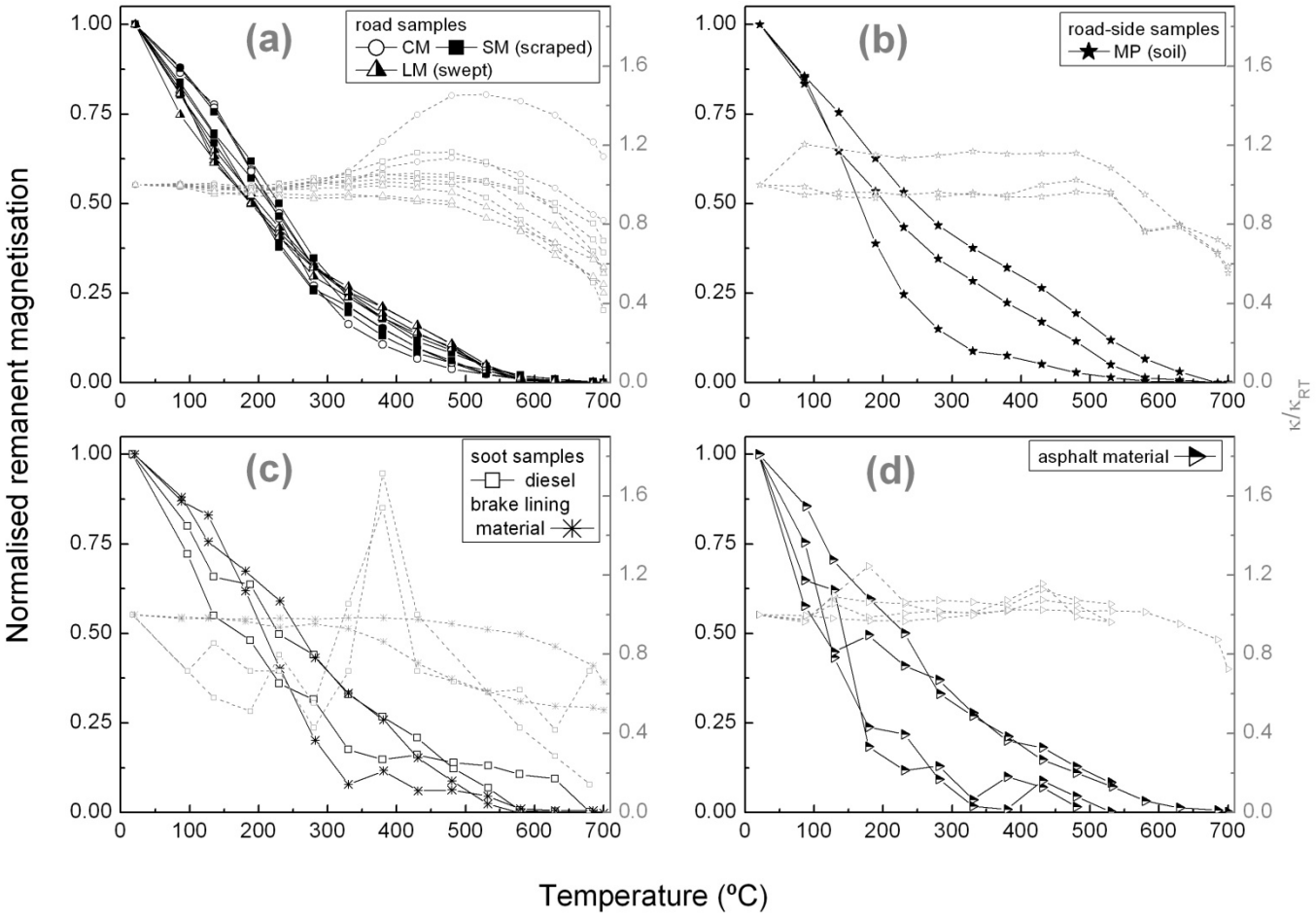
(a)
road samples
CM
SM (scraped)
LM (swept)
(b)
road-side samples
MP (soil)
(c)
soot samples
diesel
brake lining material
(d)
asphalt material
Normalised remanent magnetisation
κ/κRT
Temperature (ºC)

Fig. 5

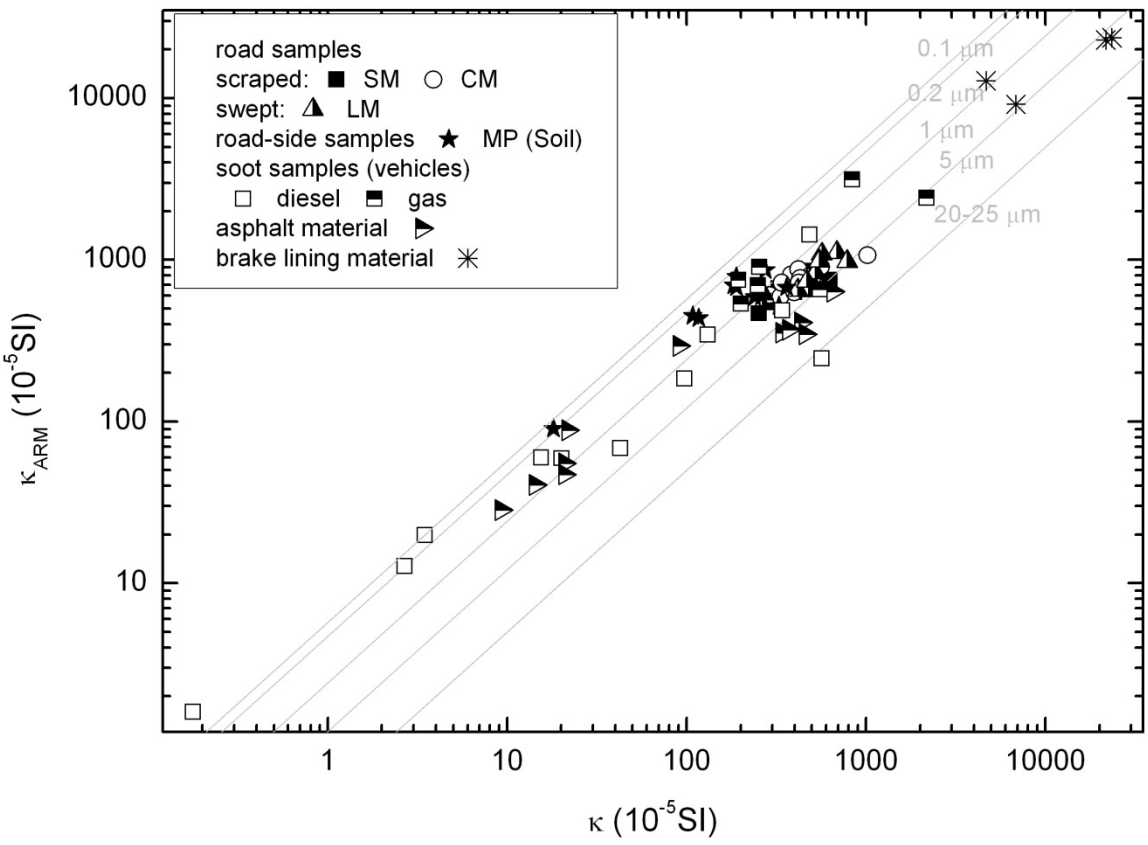
road samples
scraped: SM CM
swept: LM
road-side samples MP (Soil)
soot samples (vehicles)
diesel gas
asphalt material
brake lining material
0.1 µm
0.2 µm
1 µm
5 µm
20-25 µm
10000
1000
100
10
1
10
100
1000
10000
κ (10-5SI)
κARM (10-5SI)

Fig. 6

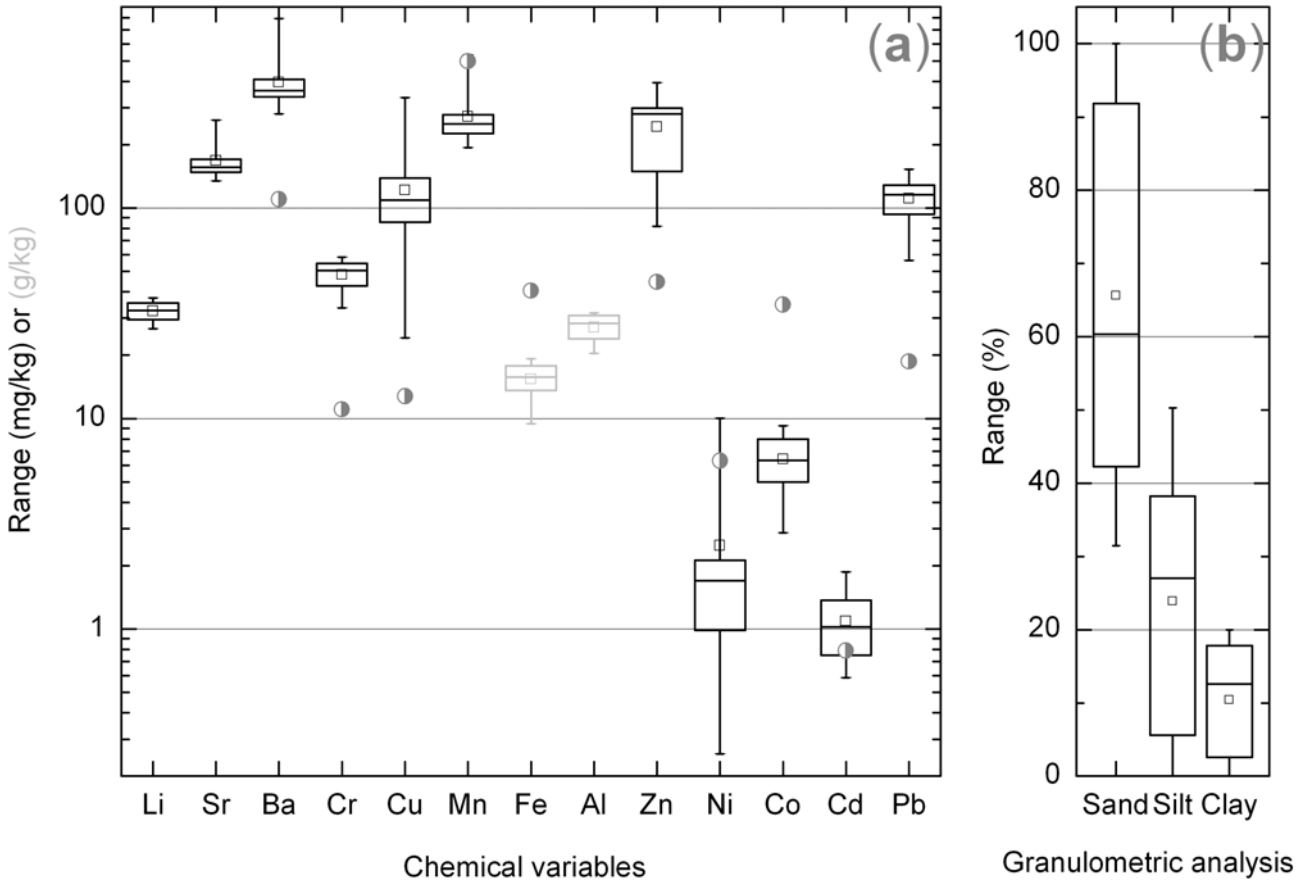
(a)
(b)
Range (mg/kg) or (g/kg)
100
10
1
Li
Sr
Ba
Cr
Cu
Mn
Fe
Al
Zn
Ni
Co
Cd
Pb
Chemical variables
Range (%)
100
80
60
40
20
0
Sand
Silt
Clay
Granulometric analysis

Fig. 7

Table 1. Statistical results (*n= 12*). Linear correlation (R-values) between magnetic and chemical variables

	κ	ARM	SIRM	H_{CR}	S-ratio	SIRM/κ	κ_{ARM}/κ
Li	**0.589**	**0.731**	0.137	0.320	-0.040	**-0.706**	0.296
K	0.367	0.418	0.414	0.461	-0.180	-0.118	-0.446
Na	0.330	0.340	0.027	0.364	-0.230	-0.443	0.064
Mg	0.351	0.366	0.058	0.286	0.337	-0.445	-0.104
Ca	0.071	0.080	0.363	0.396	**0.586**	0.276	**-0.529**
Sr	0.007	0.151	**0.557**	0.383	**0.571**	**0.545**	**-0.635**
Ba	-0.421	**-0.568**	-0.403	-0.152	0.263	0.149	-0.184
Cr	**0.775**	**0.833**	0.464	0.433	-0.217	**-0.564**	0.113
Cu	-0.203	-0.128	0.086	0.112	-0.269	0.425	0.275
Mn	0.341	**0.510**	**0.757**	**0.629**	0.384	0.284	**-0.601**
Fe	**0.703**	**0.674**	0.322	0.426	-0.229	**-0.609**	0.096
Al	**0.538**	0.462	-0.114	-0.034	0.051	**-0.831**	0.347
Zn	0.195	0.196	-0.248	0.078	-0.487	-0.494	**0.630**
Ni	-0.159	-0.065	0.161	0.132	-0.148	0.450	0.352
Co	**0.645**	**0.564**	0.056	0.280	-0.295	**-0.816**	0.225
Cd	**0.693**	**0.730**	0.285	0.042	-0.162	**-0.640**	0.189
Pb	0.242	0.207	-0.075	-0.197	-0.361	-0.335	**0.554**